Supplementary material: Water diffusion mechanisms in bitumen studied through molecular dynamics simulations

Lili Ma[a], Hirad S. Salehi[b], Ruxin Jing[a], Sandra Erkens[a], Thijs J. H. Vlugt[b], Othonas A. Moultos[b,*], Michael L. Greenfield[c,*], Aikaterini Varveri[a]

[a]*Department of Engineering Structures, Faculty of Civil Engineering and Geosciences, Delft University of Technology, Delft, Netherlands*
[b]*Engineering Thermodynamics, Process & Energy Department, Faculty of Mechanical, Maritime and Materials Engineering, Delft University of Technology, Delft, Netherlands*
[c]*Department of Chemical Engineering, University of Rhode Island, Rhode Island, United States*

This supplementary material presents descriptions of force field parameters, molecular structures, simulation details, and supporting results.

The OPLS-AA force field [1, 2, 3] was used to model inter- and intramolecular interactions within the AAA-1 bitumen model [4]. The contributions of bond stretching, angle bending, torsion, and improper torsion, as well as non-bonded terms (i.e. Lennard-Jones (LJ) and Coulomb interactions) were calculated on the basis of equations S1 to S6, shown in section 1. Long-range electrostatic interactions were computed via the Particle-Particle Particle-Mesh (PPPM) method with a relative precision of 10^{-5}. The SPC/E model was used for water. The RATTLE extension [5] of the SHAKE algorithm [6] was used to fix the bond lengths and angles of water molecules. The force field parameters of all molecules in the AAA-1 bitumen model were obtained from prior work [4], which contains standard OPLS-AA parameters reported in the literature [1, 7] and quantum mechanics-based parameters for certain functional groups that are not available elsewhere in the literature. All force field parameters of bitumen molecules are listed in Tables S1 to S5. Water parameters are listed in Table S6.

The 12-component, AAA-1 bitumen model with 72 molecules (5572 atoms in total) [4] was used to represent the saturates, aromatics, resins, and asphaltenes in bitumen. The asphaltene molecules are asphaltene-phenol, asphaltene-pyrrole, and asphaltene-thiophene; the resin molecules are benzobisbenzothiophene, pyridinohopane, quinolinohopane, thio-isorenieratane, and trimethylbenzene-oxane; the aromatic molecules are perhydrophenanthrene-naphthalene (PHPN), and dioctyl-cyclohexane-naphthalene (DOCHN); the saturate molecules are squalane and hopane. The detailed molecular structures and atom labels of asphaltenes and resins are presented in Figures S1 to S8. Rules for labeling atoms in aromatics and saturates are identical to those shown in Figures S1 to S8. The molecular structure of water is depicted in Figure S9. The detailed composition of AAA-1 bitumen model is shown in Table S7 and the simulation times of water-bitumen systems at various temperatures are listed in Table S8. Mean-squared displacements (MSDs) of integrated stress that are used to determine viscosity at temperatures from 533 K to 353 K are shown in Figures S10 to S13.

*Corresponding author
Email addresses: O.Moultos@tudelft.nl (Othonas A. Moultos), greenfield@uri.edu (Michael L. Greenfield)

1. OPLS-AA Force field parameters

The standard 12/6 Lennard-Jones potential energy describes the potential energy of interaction between two non-bonding atoms as

$$E_{\mathrm{LJ}} = 4\epsilon\left[\left(\frac{\sigma}{r}\right)^{12} - \left(\frac{\sigma}{r}\right)^{6}\right] \quad r < r_{\mathrm{c}} \tag{S1}$$

where r is the distance between atoms and r_{c} is the cutoff.

Coulombic pairwise interaction energy is given by

$$E_{\mathrm{col}} = \frac{Cq_iq_j}{r} \quad r < r_{\mathrm{c}} \tag{S2}$$

where r_{c} is the cutoff. Coulombic interaction beyond the cutoff, i.e., the long-range Coulombic energy, is computed by the PPPM method.

The bond stretching energy is described by the harmonic style,

$$E_{\mathrm{bond}} = K_{\mathrm{r}}(r - r_0)^2 \tag{S3}$$

where r_0 is the equilibrium bond distance and K_{r} is a pre-factor.

The harmonic angle bending energy is computed by

$$E_{\mathrm{angle}} = K_\theta(\theta - \theta_0)^2 \tag{S4}$$

where θ is the bond angle, θ_0 is the equilibrium value of the angle, and K_θ is a pre-factor. Angle differences are computed within LAMMPS in radians.

The dihedral energy uses the potential

$$E_{\mathrm{dihedral}} = \frac{1}{2}K_1[1 + \cos(\phi)] + \frac{1}{2}K_2[1 - \cos(2\phi)] + \frac{1}{2}K_3[1 + \cos(3\phi)] \tag{S5}$$

where K_1, K_2, and K_3 are pre-factors, and ϕ is the dihedral angle.

The improper energy is computed by

$$E_{\mathrm{improper}} = K[1 + d\cos(n\phi)] \tag{S6}$$

where ϕ is the improper angle, d equals +1 or -1, and K is a pre-factor.

Table S1 Non-bonded parameters for Equation S1 and atoms of bitumen.

Atom type	ϵ/[kcal·mol^{-1}]	σ/[Å]
CA	0.07	3.55
CS	0.07	3.55
CT	0.066	3.5
CW	0.07	3.55
CX	0.07	3.55
CY	0.07	3.55
H	0	0
HA	0.03	2.42
HC1	0.03	2.5
HO	0	0
NA	0.17	3.25
NC	0.17	3.25
OHp	0.17	3.07
OS	0.14	2.9
SA	0.25	3.55

Atom labels are denoted in Figures S1 to S8.

Table S2 Bond parameters for Equation S3.

Bond type	K_r/[kcal·mol^{-1} · Å^{-2}]	r_0/[Å]
CA-CA	469	1.4
CA-CS	546	1.382
CA-CT	317	1.51
CA-CW	546	1.367
CA-CX	469	1.409
CA-CY	410	1.394
CA-HA	367	1.08
CA-NC	483	1.339
CA-OHp	450	1.364
CA-OS	364	1.38
CS-CS	469	1.424
CS-CT	317	1.51
CS-CW	546	1.367
CS-HA	367	1.08
CT-CT	268	1.529
CT-CW	317	1.504
CT-HC1	340	1.09
CT-OS	320	1.41
CW-HA	367	1.08
CW-NA	427	1.381
CW-SA	340	1.71
CX-CX	400	1.4653
CX-CY	447	1.415
CY-SA	340	1.76
H-NA	434	1.01
HO-OHp	553	0.945

Table S3 Angle parameters for Equation S4.

Angle type	K_θ/[kcal·mol^{-1} · rad^{-2}]	θ_0/[deg]
CA-CA-CA	63	120
CA-CA-CS	70	110.6
CA-CA-CT	70	120
CA-CA-CW	35	107.4
CA-CA-CX	80	120.6
CA-CA-CY	70	117.9507
CA-CA-HA	35	120
CA-CA-NC	70	124
CA-CA-OHp	70	120
CA-CA-OS	66.1	122.03
CA-CS-CS	70	110.6
CA-CS-CW	70	110.6
CA-CT-CT	63	114
CA-CT-HC1	35	109.5
CA-CW-CS	70	110.6
CA-CW-NA	70	109
CA-CW-SA	70	110.6
CA-CX-CX	70	130.9364
CA-CX-CY	85	117.0542
CA-CY-CX	85	122.5475
CA-CY-SA	70	124.6906
CA-NC-CA	70	117
CA-OHp-HO	35	113
CA-OS-CT	60	117
CS-CS-CT	70	107.3
CS-CS-CW	70	107.3
CS-CS-HA	35	127.5
CS-CT-HC1	70	110.6
CS-CW-CT	70	121.6
CS-CW-HA	35	132.1
CS-CW-NA	70	107.7
CS-CW-SA	70	110.6
CT-CA-CW	70	110.6
CT-CA-NC	70	116
CT-CS-CW	70	110.6
CT-CT-CT	58.35	112.7
CT-CT-CW	63	114
CT-CT-HC1	37.5	110.7
CT-CT-OS	50	109.5
CT-CW-SA	70	121.6
CW-CA-HA	35	126.9
CW-CS-HA	35	125.7
CW-CT-HC1	35	109.5
CW-NA-CW	70	109.8
CW-NA-H	35	120
CW-SA-CW	70	92.2
CX-CA-CY	80	120.6
CX-CA-HA	70	120.8436
CX-CX-CY	63	111.1594
CX-CY-SA	100	112.7619
CY-CA-HA	35	120.519
CY-SA-CY	70	90.8123
HA-CW-NA	35	121.6
HC1-CT-HC1	33	107.8

Table S4 Dihedral parameters for Equation S5.

Dihedral type	K_1/[kcal/mol]	K_2/[kcal/mol]	K_3/[kcal/mol]
CA-CA-CA-X	0	7.25	0
CA-CA-CS-X	0	7.25	0
CA-CA-CT-X	0	0	0
CA-CA-CW-X	0	7.25	0
CA-CA-CX-X	0	7.25	0
CA-CA-CY-X	0	7.25	0
CA-CA-NC-CA	0	7.25	0
CA-CA-OHp-HO	0	1.682	0
CA-CA-OS-CT	0	2.200135	0
CA-CS-CS-X	0	7.25	0
CA-CS-CW-X	0	7.25	0
CA-CT-CT-CA	-2.06	-0.313	0.315
CA-CT-CT-CT	0	0	0.366
CA-CT-CT-HC1	0	0	0.462
CA-CW-NA-CW	0	3.2	0
CA-CW-NA-H	0	3.2	0
CA-CW-SA-CW	0	7.25	0
CA-CX-X-X	0	7.25	0
CA-CY-SA-CY	0	7.25	0
CS-CA-CA-CT	0	7.25	0
CS-CS-CT-HC1	1.876	0	0
CS-CS-X-X	0	7.25	0
CS-CW-NA-CW	0	3.2	0
CS-CW-NA-H	0	3.2	0
CS-CW-SA-CW	0	7.25	0
CT-CA-X-X	0	7.25	0
CT-CS-X-X	0	7.25	0
CT-CT-CT-CT	1.74	-0.157	0.279
CT-CT-CT-CW	1.876	0	0
CT-CT-CT-HC1	0	0	0.366
CT-CT-CT-OS	-1.336	0	0
CT-CT-CW-CS	1.876	0	0
CT-CT-CW-SA	1.876	0	0
CT-CT-OS-CA	-3.7	1.867983	0.938689
CT-CW-SA-CW	0	7.25	0
CW-CA-CA-HA	0	7.25	0
CW-CA-CT-CT	0	0	0
CW-CA-CT-HC1	-7.582	3.431	3.198
CW-CS-CS-CW	0	7.25	0
CW-CS-CS-HA	0	7.25	0
CW-CS-CT-HC1	1.876	0	0
CW-CT-CT-HC1	0	0	0.462
CX-CA-X-X	0	7.25	0
CX-CX-CY-X	0	7.25	0
CX-CY-SA-CY	0	7.25	0
CY-CA-X-X	0	7.25	0
CY-CX-CX-CY	0	7.25	0
HA-CA-X-X	0	7.25	0
HA-CS-X-X	0	7.25	0
HA-CW-NA-X	0	3.2	0
HC1-CT-CT-HC1	0	0	0.318
HC1-CT-CT-OS	0	0	0.468
HC1-CT-CW-X	1.876	0	0
NC-CA-CT-X	0	0	0

An X represents any other atom type (“wild”).

Table S5 Improper parameters for Equation S6.

Improper type	K/[kcal/mol]	d	n
CA-CA-CA-CA	1.1	-1	2
CA-CA-CA-CS	1.1	-1	2
CA-CA-CA-CT	1.1	-1	2
CA-CA-CA-HA	1.1	-1	2
CA-CA-CA-NC	1.1	-1	2
CA-CA-CA-OHp	1.1	-1	2
CA-CA-CA-OS	1.1	-1	2
CA-CA-CT-CW	1.1	-1	2
CA-CA-CT-NC	1.1	-1	2
CA-CA-CW-HA	1.1	-1	2
CA-CA-CX-HA	1.1	-1	2
CA-CA-CY-HA	1.1	-1	2
CA-CX-CY-HA	1.1	-1	2
CS-CA-CS-CW	1.1	-1	2
CS-CS-CT-CW	1.1	-1	2
CS-CS-CW-HA	1.1	-1	2
CW-CA-CS-NA	1.1	-1	2
CW-CA-CS-SA	1.1	-1	2
CW-CS-CT-SA	1.1	-1	2
CW-CS-HA-NA	1.1	-1	2
CX-CA-CX-CY	1.1	-1	2
CY-CA-CX-SA	1.1	-1	2
NA-CW-CW-H	1	-1	2

Table S6 Non-bonded parameters for SPC/E water model.

Atom	ϵ/[kcal/mol]	σ/[Å]	q/[e^-]
H	0.1553	3.166	0.4238
O	0.0	0.0	-0.8476

2. Molecular structures and labeling of atoms

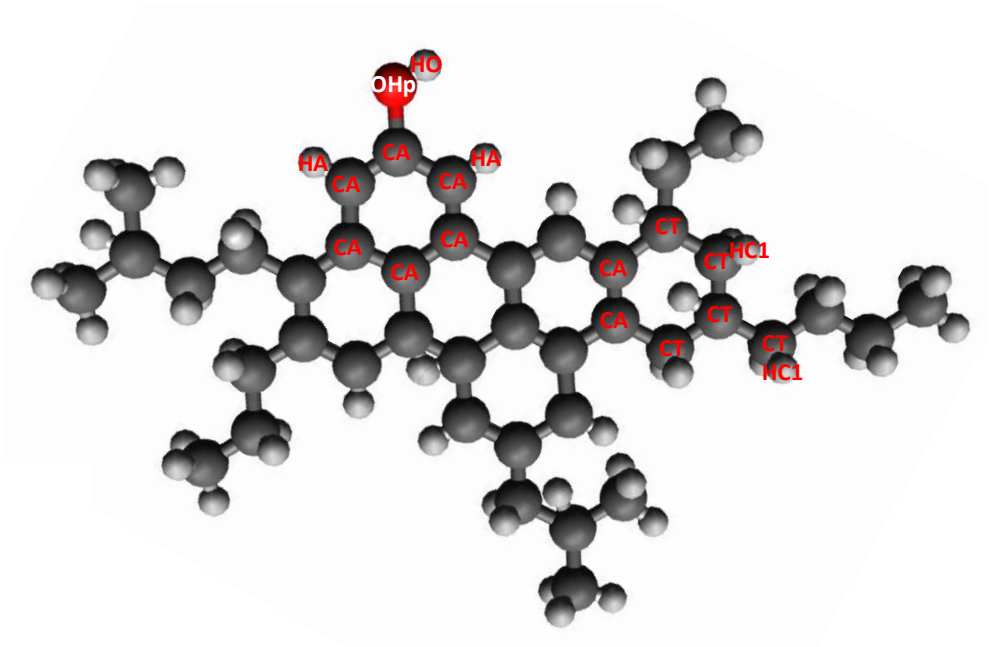

Fig. S1. Structure of asphaltene-phenol. Colors for carbon, hydrogen, nitrogen, oxygen, and sulfur are dark gray, light gray, blue, red, and yellow, respectively.

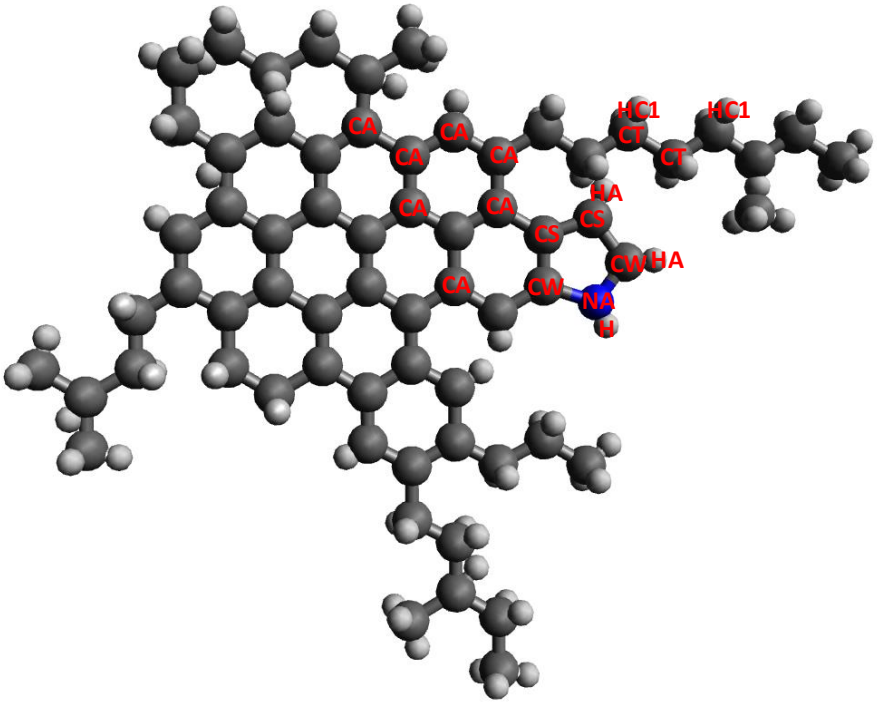

Fig. S2. Structure of asphaltene-pyrrole.

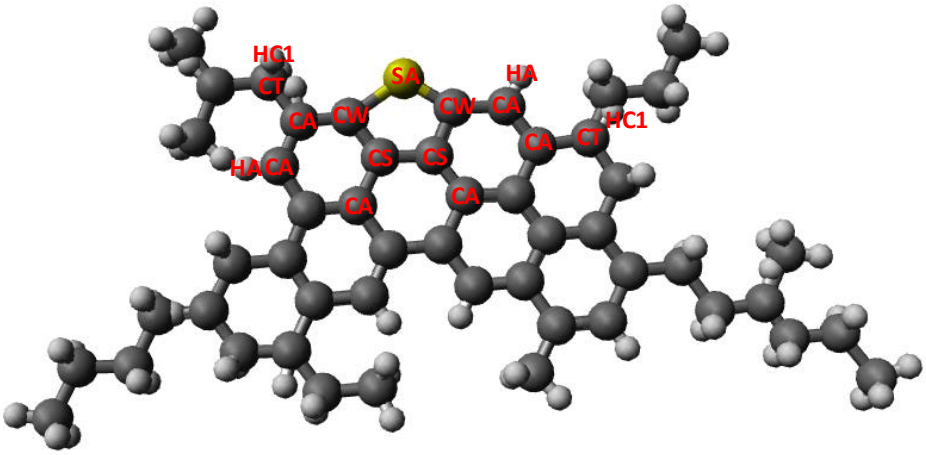

Fig. S3. Structure of asphaltene-thiophene

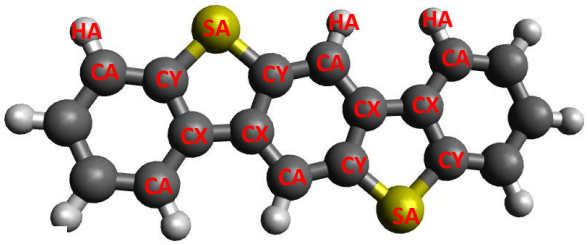

Fig. S4. Structure of benzobisbenzothiophene

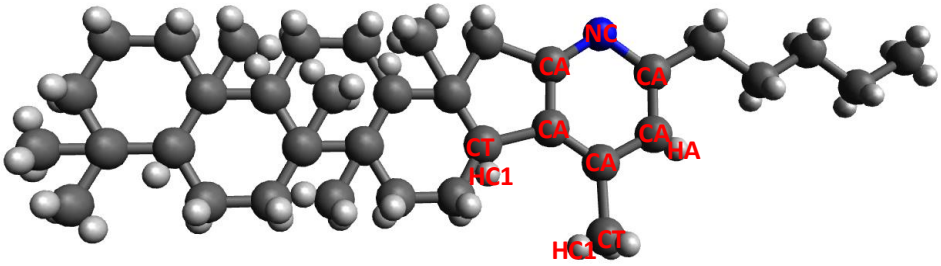

Fig. S5. Structure of pyridinohopane with torsion angles within saturated rings chosen to emphasize legibility rather than high probability

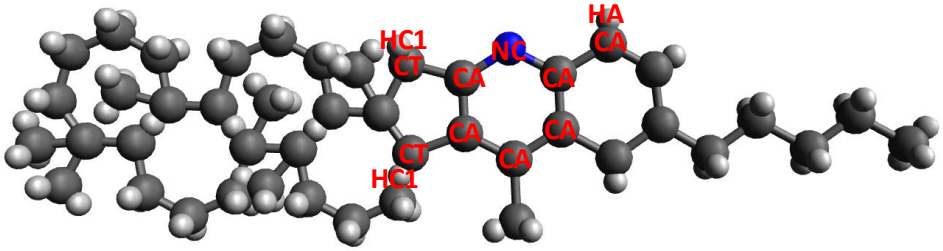

Fig. S6. Structure of quinolinohopane with torsion angles as in Figure S5

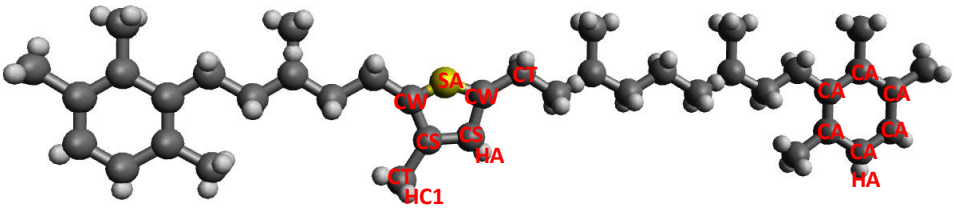

Fig. S7. Structure of thio-isorenieratane

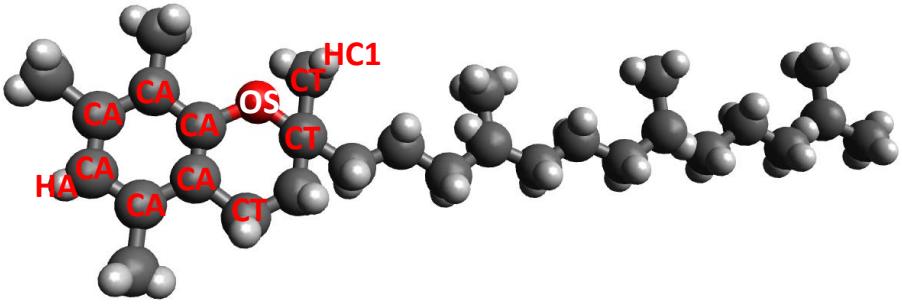

Fig. S8. Structure of trimethylbenzene-oxane

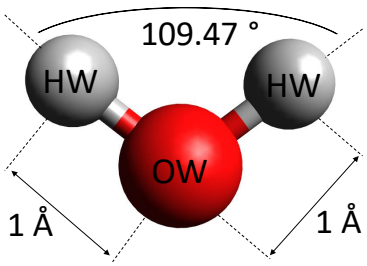

Fig. S9. Structure of water

Table S7 Bitumen composition

Molecule	Number in the system	Molar mass (g/mol)
asphaltene-phenol	3	575.0
asphaltene-pyrrole	2	888.5
asphaltene-thiophene	3	707.2
benzobisbenzothiophene	15	290.4
pyridinohopane	4	530.9
quinolinohopane	4	554.0
thio-isorenieratane	4	573.1
trimethylbenzene-oxane	5	414.8
perhydrophenanthrene-naphthalene (PHPN)	11	464.8
dioctyl-cyclohexane-naphthalene (DOCHN)	13	406.8
squalane	4	422.9
hopane	4	483.0

3. Simulation run time details

Table S8 Details of simulation times

Temperature/[K]	NPT equilibration /[ns]	NVT equilibration /[ns]	NVT production /[ns]
533	1	1	10
443	10	2	100
393	20	10	100
353	20	10	300
313	50	10	600
298	80	10	600

4. Trajectories of water clusters that involve molecule 10

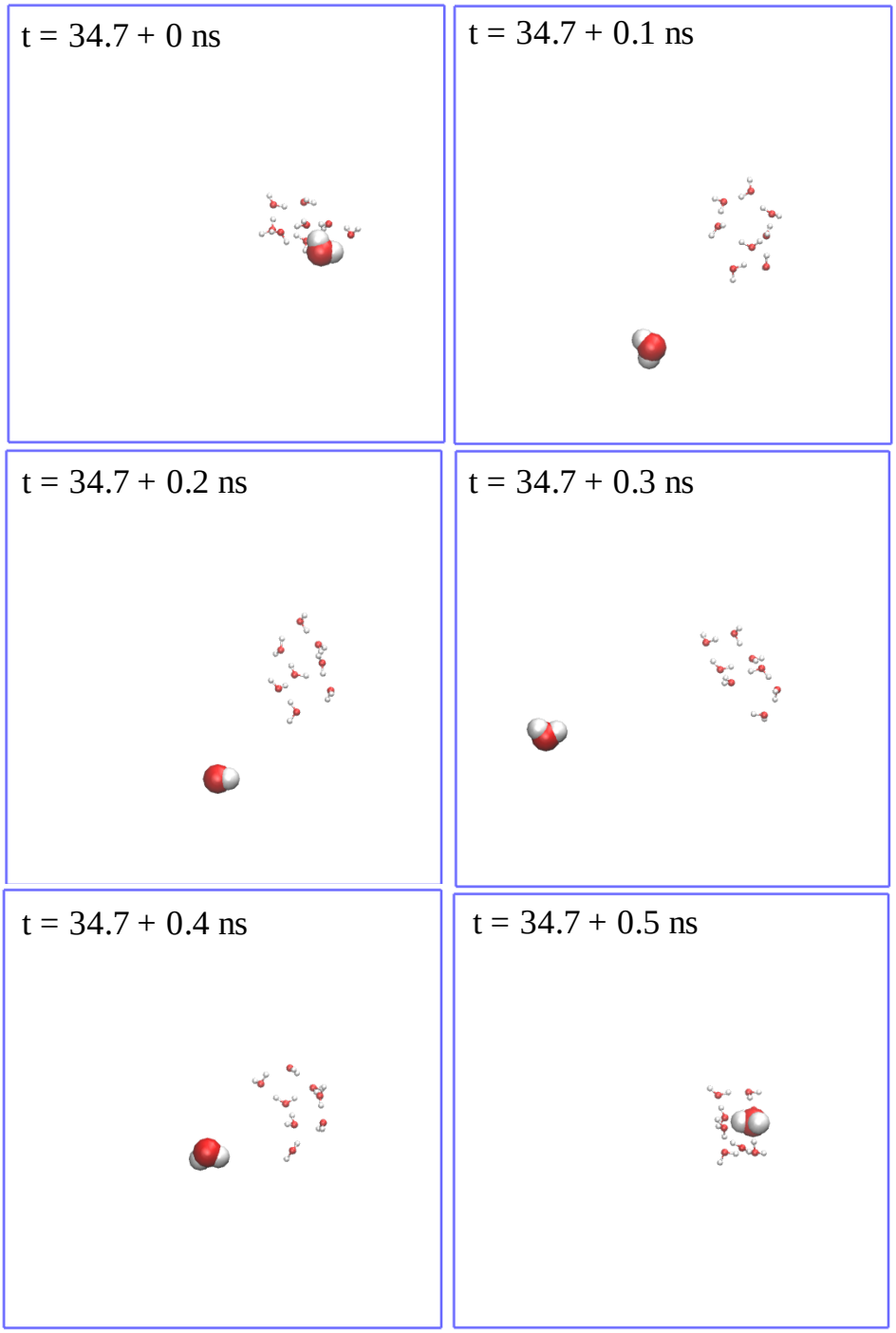

Fig. S10. Continuous trajectory snapshots (with an interval of 100 ps) of molecule 10 and cluster group 1 in the bitumen system with 16 water molecules (0.93 wt% water content) at 313 K. Molecules with smaller radii represent water cluster group 1 while molecule 10 is depicted with a larger radius.

5. MSDs that lead to viscosity

The OCTP plugin [8] in LAMMPS was used for the on-the-fly calculation of the MSDs of viscosity:

$$\mathrm{MSD} = \frac{1}{10 \cdot 2}\frac{V}{k_\mathrm{B}}\left\langle \sum_{\alpha\beta}\left(\int_0^t P^{\mathrm{os}}_{\alpha\beta}(t')\,\mathrm{d}t'\right)^2\right\rangle \tag{S7}$$

where

$$P^{\mathrm{os}}_{\alpha\beta} = \frac{P_{a\beta} + P_{\beta a}}{2} - \delta_{\alpha\beta}\left(\frac{1}{3}\sum_k P_{kk}\right) \tag{S8}$$

and V is the volume of the system, $P^{\mathrm{os}}_{\alpha\beta}$ are the traceless pressure tensor components, t is the correlation time, k_B is the Boltzmann constant, and $\delta_{\alpha\beta}$ is the Kronecker delta. Markers $\langle\ \rangle$ denote an ensemble average.

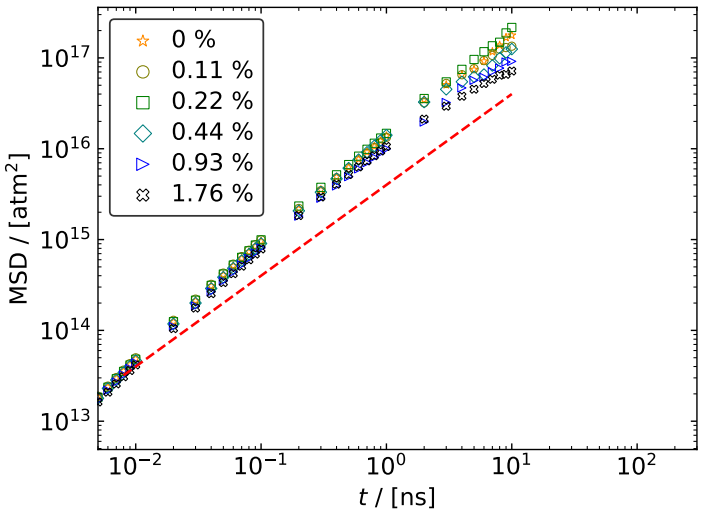

Fig. S11. MSD of stress fluctuations at 533 K. The slope of the red dashed line is 1.

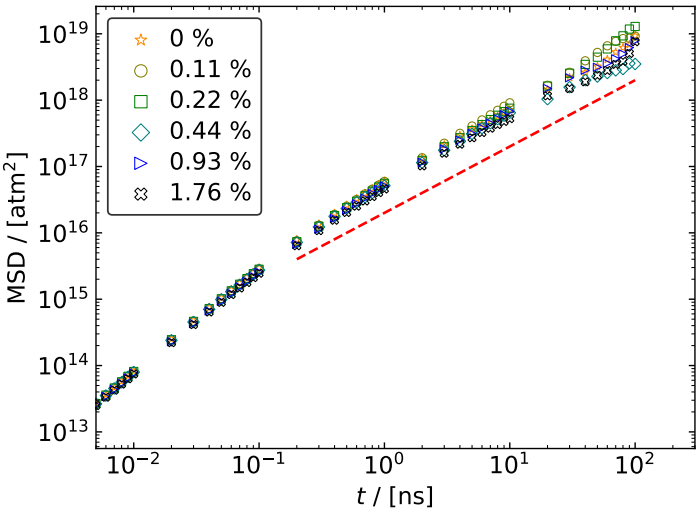

Fig. S12. MSD of viscosity at 443 K. The slope of the red dashed line is 1.

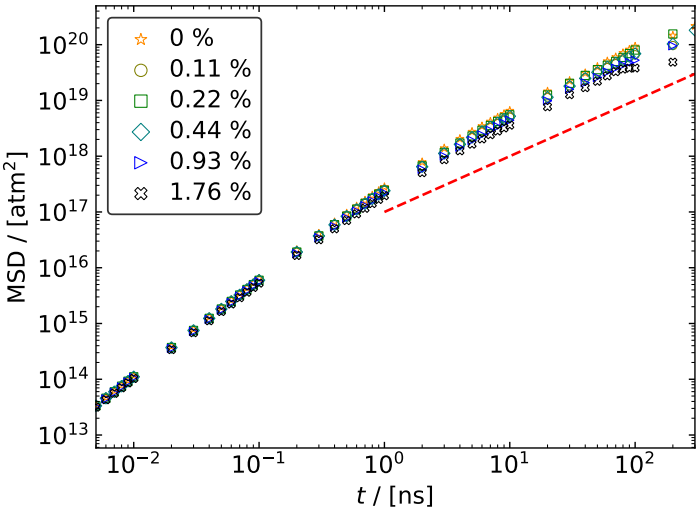

Fig. S13. MSD of viscosity at 393 K. The slope of the red dashed line is 1.

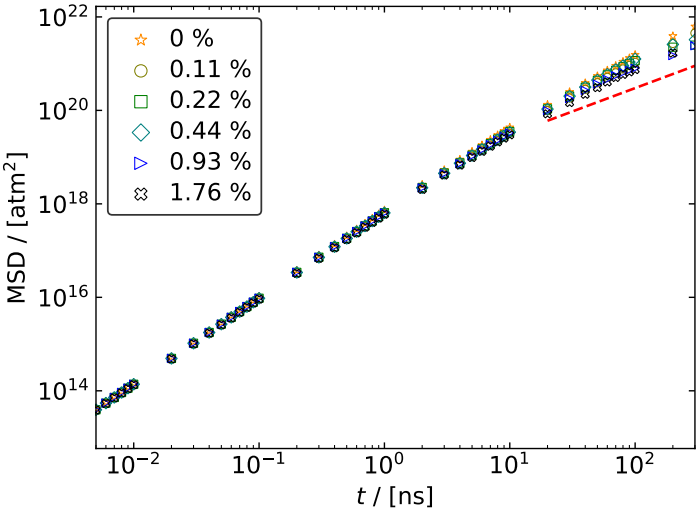

Fig. S14. MSD of viscosity at 353 K. The slope of the red dashed line is 1.

References

[1] W. L. Jorgensen, D. S. Maxwell, J. Tirado-Rives, Development and testing of the OPLS all-atom force field on conformational energetics and properties of organic liquids, Journal of the American Chemical Society 118 (45) (1996) 11225–11236.

[2] M. G. Martin, J. I. Siepmann, Transferable potentials for phase equilibria. 1. united-atom description of *n*-alkanes, The Journal of Physical Chemistry B 102 (14) (1998) 2569–2577.

[3] M. L. P. Price, D. Ostrovsky, W. L. Jorgensen, Gas-phase and liquid-state properties of esters, nitriles, and nitro compounds with the OPLS-AA force field, Journal of Computational Chemistry 22 (13) (2001) 1340–1352.

[4] D. D. Li, M. L. Greenfield, Chemical compositions of improved model asphalt systems for molecular simulations, Fuel 115 (2014) 347–356.

[5] H. C. Andersen, Rattle: A "velocity" version of the shake algorithm for molecular dynamics calculations, Journal of Computational Physics 52 (1) (1983) 24–34.

[6] J.-P. Ryckaert, G. Ciccotti, H. J. Berendsen, Numerical integration of the cartesian equations of motion of a system with constraints: molecular dynamics of *n*-alkanes, Journal of Computational Physics 23 (3) (1977) 327–341.

[7] G. A. Kaminski, R. A. Friesner, J. Tirado-Rives, W. L. Jorgensen, Evaluation and reparametrization of the OPLS-AA force field for proteins via comparison with accurate quantum chemical calculations on peptides, The Journal of Physical Chemistry B 105 (28) (2001) 6474–6487.

[8] S. H. Jamali, L. Wolff, T. M. Becker, M. De Groen, M. Ramdin, R. Hartkamp, A. Bardow, T. J. H. Vlugt, O. A. Moultos, OCTP: A tool for on-the-fly calculation of transport properties of fluids with the order-*n* algorithm in LAMMPS, Journal of Chemical Information and Modeling 59 (4) (2019) 1290–1294.